Proceedings of the 16th IKM 2003, Gürlebeck, Hempel, Könke (eds.), Weimar, Germany, June 10-12, 2003, ISSN 1611-4086

A geometrical inclusion-matrix model for the finite element analysis of concrete at multiple scales

Stefan Häfner, Stefan Eckardt and Carsten Könke
Institute of Structural Mechanics, Bauhaus-University Weimar, Marienstrasse 15, D-99423 Weimar, Germany

1 Motivation

The maximum size, the shapes and the size-distribution of natural aggregates within the mortar matrix significantly influence the behaviour of concrete structures. Correlations between maximum aggregate size and tensile strength, as well as fracture energy have been confirmed and quantified by experiments in Van Mier [6]. Furthermore it is obvious, that sharp edged aggregate shapes cause higher local stress concentrations than compact smooth shapes. Consequently crack initiation and crack propagation also depend on the particle shapes. The size-distribution of aggregates determines the compactibility and highest local density of particles. For reliable prediction of the structural behaviour and damage evolution of concrete, these local effects caused by the particles are included into the computational structural analysis.

2 The Geometrical Model

Independent of a numerical discretization an adequate geometrical inclusion-matrix model of concrete is created. Therefore particle shapes, particle size distribution functions, the generation of particle arrangements and simulation aspects are considered.

2.1 Particle Shapes

The natural aggregates significantly influence the local stress distribution on the mesoscopic level. Cracks initiate and propagate on this length scale within the most often weaker matrix material. The shape of the inclusions has an effect on the local stresses and therewith influences the crack path. However, cracking of the natural aggregates is also observed and should be included with respect to the corresponding particle strength properties. It is obvious, that a two-dimensional formulation of the inclusions can not represent the real three-dimensional situation. Nebertheless as a first step ellipses where considered, which have the advantage of a very simple formulation and allow for a closed form analysis. The general ellipse is described by five independent parameters: the radii r_1 and r_2, the center coordinates c_x and c_y, and the rotation angle α (Fig. 1). Translation and rotation of the basic ellipse equation

$$\left(\frac{x}{r_1}\right)^2 + \left(\frac{y}{r_2}\right)^2 - 1 = 0 \tag{1}$$

lead to the polynomial formulation

$$c_1 x^2 + c_2 x + c_3 xy + c_4 y + c_5 y^2 + 1 = 0 \tag{2}$$

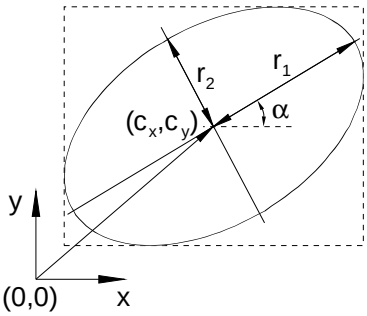

Figure 1: Geometry, parameters and bounding box of the general ellipse

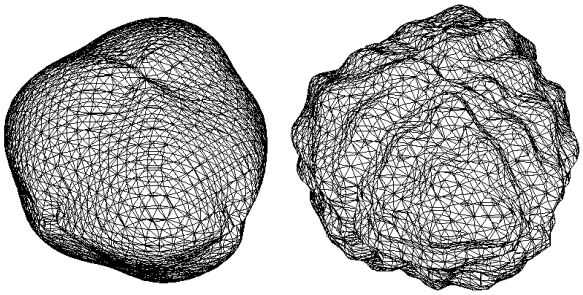

Figure 2: Particles shapes generated by adding sinus functions on ellipsoid

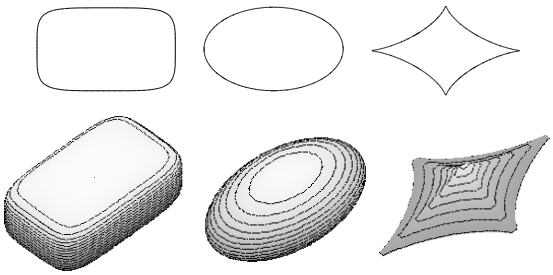

Figure 3: Shapes of the polynomial function with exponent n=5, 2 and 0.7

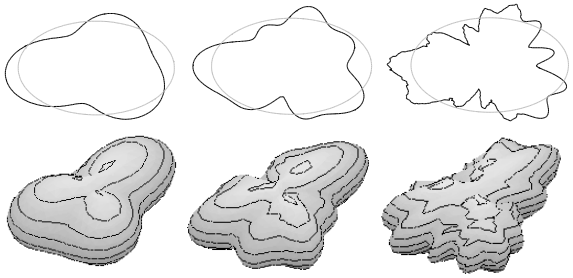

Figure 4: Incremental addition of sinus functions on polynomial function (n=2)

with a corresponding parameter set of $c_1 \dots c_5$. Whereas the first parameter set is useful to control the volume and fast approximation of location the latter ones are used for an accurate seperation check. Correspondingly there are nine parameters for the ellipsoid: r_1, r_2, r_3, c_x, c_y, c_z, the Eulerian angles θ, ψ, ϕ, and the following polynomial function:

$$c_1x^2 + c_2y^2 + c_3z^2 + c_4xy + c_5xz + c_6yz + c_7x + c_8y + c_9z + 1 = 0 \tag{3}$$

A disadvantage of the ellipse is, that with their ideally smooth shape stress concentrations at angular surfaces of the real material are neglected. A more general formulation of the basic ellipsoid function by varying the exponent allows for several different shapes and is demonstrated by Zohdi [9],

$$\left|\frac{x}{r_1}\right|^n + \left|\frac{y}{r_2}\right|^n + \left|\frac{z}{r_3}\right|^n - 1 = 0 \tag{4}$$

but still appears to be restrictive (Fig. 3). Koensler [3] assembles results from Krumbein and Sloss, who analyze and categorize shapes of natural aggregates in terms of sphericity and angularity, as well as from Russel, Taylor and Pettijohn, who differentiate among angular, subangular, subrounded, rounded and well rounded aggregates. The intuitive extension of the polynomial formulation (Eq. 1) by a sum of sine functions F_i of varying periodic repetitions $p_i \in \mathbf{N}$, particle size scaled amplitude A_i and an initial value e_i for rotation theoretically allows for a wide variety of shapes (Fig. 4, top):

$$F_i = A_i \cdot \sin(\arctan\left(\frac{y}{x}\right) \cdot p_i + e_i) \tag{5}$$

The terms F_i can also be applied to Equation 4 (Fig. 4, bot.) and further be transfered to three dimensional coordinates (Fig. 2). However, in further research it is useful to develope a statistical description of these parameters meeting the different categories and translate them to practical terms as rounded, angular, cubical shaped and laminated. Within the framework of Revitalization of Buildings[1] it is useful to identify the shape parameters of the existing mesoscale geometry by analyzing section surfaces or using non-destructive techniques.

[1] Sonderforschungsbereich 524 at Bauhaus-University Weimar

2.2 The Generation of a Two-Dimensional Inclusion-Matrix Model

The use of a two-dimensional inclusion-matrix model to predict the structural response of concrete is rather questionable and it is even not clear, if it should either represent an arbitrary section of the three-dimensional body or a designed particle size distribution mapped onto a plane. Furthermore the volume fraction of aggregates can not directly be transfered from three to two dimensions. Besides it might still be useful for some applications, it is well suitable as working model for developing the principle algorithm and the following conclusions were drawn:

- It is useful to generate the complete set of particles up to the required volume fraction by Monte-Carlo Simulation on the inverse cumulative particle size distribution function in advance to assure a consistent representation of particle sizes.

- For randomly finding valid particle positions, sorting all particles by size and starting with the largest particle to be located in the domain drastically improves simulation efficiency and supports a successful particle packing result (Fig. 5)

- It is useful, to combine very fast seperation checks of particles, like partitioning into subdomains or just comparing bounding boxes of particles, with accurate seperation checks based on a analytical formulation or based on a numerical scan algorithm of the surfaces in the region of overlapping bounding boxes. The latter one then can also be applied to arbitrary particle shapes on the condition that reasonable tight bounding boxes have been determined in advance.

2.3 A Heuristic Compaction Algorithm (2D)

For achieving very dense particle arrangements an additional compaction algorithm was introduced, which results from the imagination of shaking the domain. Based on a globally adapting step size all particles are at once tested for an incremental movement either to the right, to the left, up or down, always given a random, particle individual direction variance of up to 45 degrees. Compaction is then achieved by a higher repetition of the sequence towards the prefered direction (e.g. down). Here always dependant on the next sequence the particles are sorted by coordinates for a higher mobility towards the next direction. The global movement stepsize is increased if more than a certain percentage (e.g. 80%) of particles were able to move, or decreased if these were less than a certain limit (e.g. 20%). It is considered as advantageous that this algorithm forces to pack the particles tighter, without necessarily pushing them towards contact. Unequal distributions can be compensated by ran-

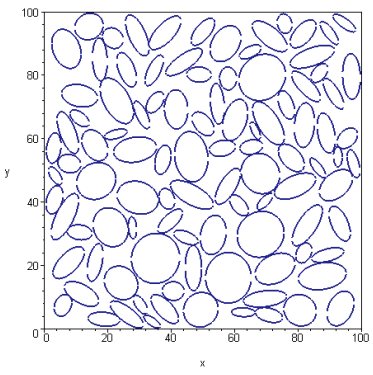

Figure 5: Sample extract of 100 inclusions (Vol. 54.4%)

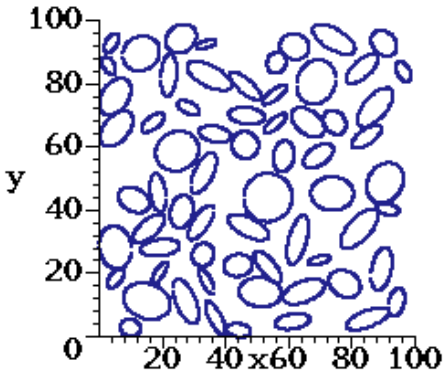

Figure 6: Sample extract of 65 inclusions (Vol. 37.9%)

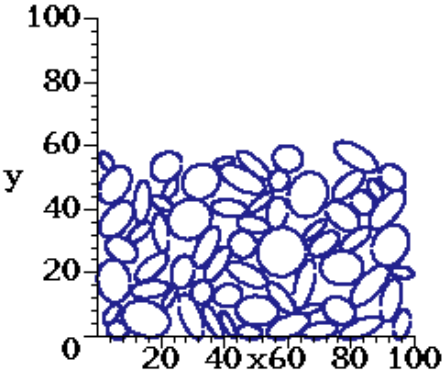

Figure 7: Inclusions of Fig. 6 after 60 iterations of compaction

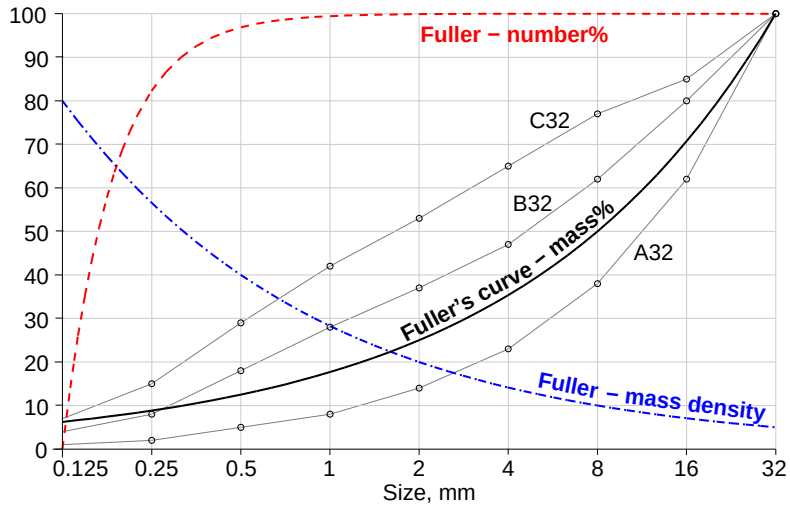

Mass[%]	2.6	3.7	5.2	7.3	10.4	14.6	20.8	29.3
Number	7043638	1245151	220114	38910	6879	1216	215	38

Figure 8: Fuller's curve and limiting grading curves in accordance with DIN 1045. Table: Number of particles in 1.36 kg aggregates for a $0.1 \cdot 0.1 \cdot 0.1\ m^3$ concrete cube designed after Fuller's curve (assuming 70% aggregate volume fraction and $\rho = 2400 \frac{kg}{m^3}$ aggregate density.)

domly applying sequences of different directions. This algorithm is heuristic, but shows a reasonable convergence and result for our example (Fig. 6, 7).

2.4 Particle Size Distribution and Volume Fraction

Generally the natural aggregates occupy between 60 and 90% of the total concrete volume [4]. The well known particle size distribution functions of concrete includes particle sizes between 0.125 and 16 (32 or 64) millimeters (Fig. 8). A particle size distribution curve for optimal packing of spherical shapes was developed by Fuller, which also lies in the proposed area in between the limiting grading curves A32 and B32 of DIN 1045. In practice concrete is most often designed after Fuller's curve for achieving the highest density and strength, as well as low segregation and good workability [3]. As the size scale of considerable mass ranges over two dimensions, a logarithmic scale is applied on the ordinate. The gradient of the cumulative distribution function is larger at small sizes, which is indicated by the relative mass density curve (not scaled) in the diagram (Fig. 8). Using Fuller's curve as example shows that the masses of the smallest and the largest particle lie within comparable ranges. Assuming equal density and dividing by the diameter related spherical volume, illustrates, that the number of small particles is far beyond the number of large particles. Based on an ideal representation the statistics for the particle number within a given volume can be evaluated, which is in the following shown by Fuller's curve, as cumulative distribution function of mass with respect to particle size x (here diameter of sphere) and maximum aggregate size D_{max}:

$$\Phi_{m\%}(x) = 100 \cdot \left(\frac{x}{D_{max}} \right)^{0.5} [\%] \tag{6}$$

Assuming a constant density ρ leads to a cumulative volume distribution Φ_V up to V_{total} and a corresponding gradient φ_V

$$\Phi_V(x) = V_{total} \cdot \left(\frac{x}{D_{max}} \right)^{0.5} [m^3] \tag{7}$$

$$\varphi_V(x) = \frac{d\Phi_V(x)}{dx} = \frac{0.5 \cdot V_{total}}{D_{max}^{0.5} \cdot x^{0.5}} \tag{8}$$

In the differential interval of $[x, x+dx]$ the increments of particle number and volume follow the condition:

$$\varphi_V(x)dx = \varphi_N(x)dx \cdot V(x) \tag{9}$$

Introducing the inclusion volume as $V(x) = \frac{4}{3}\left(\frac{x}{2}\right)^3 \pi$ (sphere) and assuming homogeneous density $V_{total} = \frac{m_{total}}{\rho}$ leads to the particle number gradient φ_N

$$\varphi_N(x) = \frac{\varphi_V(x)}{V(x)} = \frac{3 \cdot m_{total}}{D_{max}^{0.5} \cdot x^{3.5} \cdot \rho \cdot \pi} \tag{10}$$

Therewith the cumulative particle number from a lower boundary x_1 up to x, denoted as $\Phi_N(x)$, and the number of particles within the range of $[x_1; x_2]$, denoted as $N[x_1; x_2]$, can be written as:

$$\Phi_N(x) = \int_{x_1}^{x} \varphi_N(z)dz = \left[\frac{-1.2 \cdot m_{total}}{D_{max}^{0.5} \cdot z^{2.5} \cdot \rho \cdot \pi}\right]_{x_1}^{x} \tag{11}$$

$$N[x_1; x_2] = \frac{1.2 \cdot m_{total}}{D_{max}^{0.5} \cdot \rho \cdot \pi}\left(\frac{1}{x_1^{2.5}} - \frac{1}{x_2^{2.5}}\right) \tag{12}$$

As a defect of Fuller's curve the lower boundary x_1 of particle size should not be zero, as this leads to a infinite number of particles. For practical purpose the smallest reasonable value most probably is 0.125mm. Nevertheless, assuming an ideal representation of the given distribution the integral exactly determines the number of particles within the range $[x_1, x_2]$ and therewith it can be used to define a cumulative distribution function $\Phi_N^{[0;1]}$ for the particle number in the interval $[x_1; x_2]$

$$\Phi_N^{[0;1]}(x) = \frac{\Phi_N(x)}{N[x_1; x_2]} = \frac{\frac{1}{x_1^{2.5}} - \frac{1}{x^{2.5}}}{\frac{1}{x_1^{2.5}} - \frac{1}{x_2^{2.5}}} \tag{13}$$

The inverse formulation can be used to generate particles within the range of $[x_1; x_2]$ according to Fuller's curve by applying uniform distributed random numbers of the interval $[0; 1]$ to $\Phi_N^{[0;1]}$

$$x\left(\Phi_N^{[0;1]}\right) = \left(\frac{1}{x_1^{2.5}} - \Phi_N^{[0;1]}\left(\frac{1}{x_1^{2.5}} - \frac{1}{x_2^{2.5}}\right)\right)^{\left(-\frac{1}{2.5}\right)} \tag{14}$$

2.5 The Generation of a Three-Dimensional Inclusion-Matrix Model

For computational performance of creating the geometry and due to a computational restriction of resolution in the finite analysis, it is clear that a threshold value for the diameter has to be chosen, below which particles will not be generated. The effective volume fraction for a certain particle size intervall within a given concrete volume is evaluated by the product of the volume fraction within the distribution function and the total volume fraction of aggregates. Figure 9 shows a random arrangement of particles according to the table attached to Figure 8 for particles with diameters larger than 8mm. For achieving an adequate volume ratio of aggregates in this case the number of particles (38 and 215) was controlled, which lead to effective volume fractions in the intervals of $13.6\% : [8; 16]$ and $19.4\% : [16; 32]$ compared to a theoretical mean value of $20.8\% \cdot 0.7 = 14.6\% : [8; 16]$ and $29.3\% \cdot 0.7 = 20.51\% : [16; 32]$ (for larger sample sizes convergence towards the expected mean value

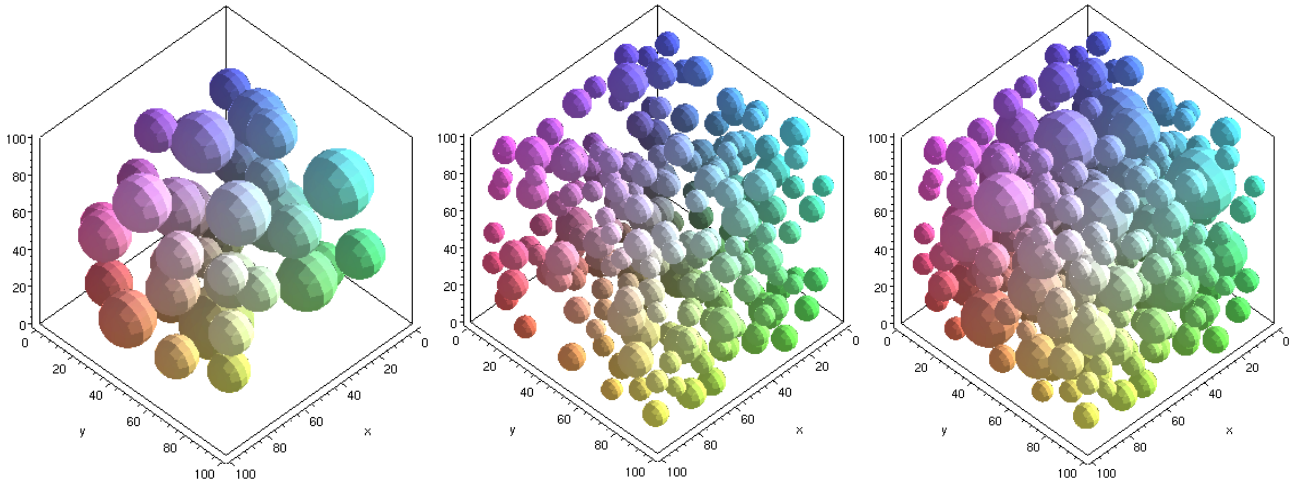

Figure 9: Particle configurations corresponding to Fuller's curve of Fig. 8: 38 particles of fraction 16-32mm, 215 particles of fraction 8-16mm and the combination of 253 particles.

was verified). In general controlling the mass rather than the number of particles is proposed and considered to be more descriptive. However, this demonstrates that the different fractions of particle sizes can be generated seperately from each other and that this concept can be adapted to other particle size distributions without the need of finding a closed form formulation over the complete particle size range. In practice, without gaining more data about the distribution within a certain fraction (between two sieve sizes), an adequate assumption has to be drawn and therefore Fuller's distribution appears to be reasonable. For a total aggregate volume of 70% the shown configuration was generated without the need of a compaction algorithm. This can be interpreted as a consequence of the ideal sieve curve, which indicates a relativly low ratio of large particles. The particles are graded by size such that in any random arrangement a dense packing can be achieved and the smaller particles can fill up the space in between the greater particles. Furtermore it is remarked and comprehensible, that there is a size effect when positioning particles within a restrictive box in terms of a relatively higher location of small particles along the boundaries depending on the box size. At next the concept has been extended for generating ellipsoidal shapes. The check of seperation of two ellipsoids is a demanding task and still an actual research object regarding efficiency. An appropriate recent theory [7] based on an algebraic condition has currently been integrated into our simulation.

2.6 Physical Properties

The geometrical arrangement as well as the physical properties of concrete are of stochastic nature. While reducing the length scale, the variances of local arrangements of different cutouts increase. Whereas homogenized mean values for the physical properties are used for analyzing the macroscopic behaviour, simulating on the mesoscale requires to account for the physical properties of the particular components. For a standard mixture of concrete Beyer [1] presents the parameters given in Table 1 and besides moreover illustrates the mechanical behaviour of concrete as two-component system on the mesoscale. Some statistics for the tensile strength of natural aggregates were observed by experiments

	Compressive Strength $[N/mm^2]$	Elastic modulus $[kN/mm^2]$
Aggregates (Quartz)	250	60
Cement stone (w/c=0.5)	25	10
Concrete B25 (DIN 1045)	30	35

Table 1: Comparison of physical properties

of a study project at Bauhaus-University Weimar [8].

As in the presented examples all particles smaller than 8mm were not modeled, the heterogeneous mortar matrix is not well presented by plain cement properties, but is ideally evaluated from homogenization of the mixture of small particles and cement. As assumption in the following numerical analysis on the defined geometries a ratio of 2 is used for the elastic moduli of inclusion and of matrix.

Concluding, a significant heterogeneous character of the geometry and physical properties is stated, which will also reflect in the mechanical analysis of the structure.

3 Finite Element Analysis of Defined Geometry

For a numerical analysis this geometrical model can be transformed into points, lines and areas, and translated to finite element codes, which offer the option of automatic mesh generation or more ambitious an own mesh generator can be designed for this problem. But whenever leaving sample sizes and modelling all surfaces of all particles, this results in many degrees of freedom and quickly leads to the limit of computation capacity. An alternative has been introduced by Zohdi and Wriggers [10], who use quadratic or cubic meshes to analyse random heterogeneous materials. Following this idea the geometry of the whole concrete structure is meshed by a uniform grid of finite elements Fig. 10-14 [2].

The different material properties are considered at each integration point by referencing the corresponding position of the geometrical model. Increasing the number of integration points leads to a higher resolution and a better representation of the heterogeneous material without increasing the number of unknowns of the finite element problem. Numerical singular corner points do not occur, as all particles' edges are smoothed through the integration points within the elements. And although not each small particle is included by any integration point the finite element response leads to a macroscopically representative solution for the linear case. This concept of modelling heterogeneous materials is clear in understanding, implementation and use.

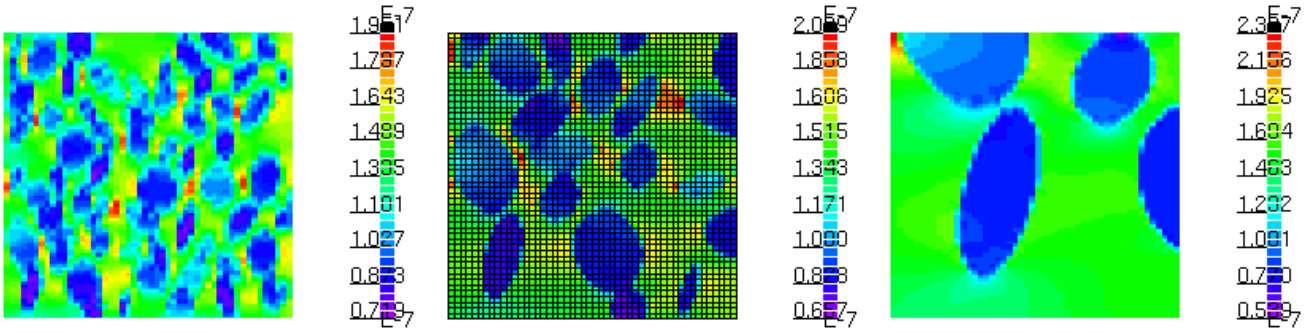

Figure 10: Strain ϵ_{xx}. Topology of 50x50 elements on square length of 100mm (a), 50mm (b) and 25mm (c) for a constant, external applied tension in x-direction.

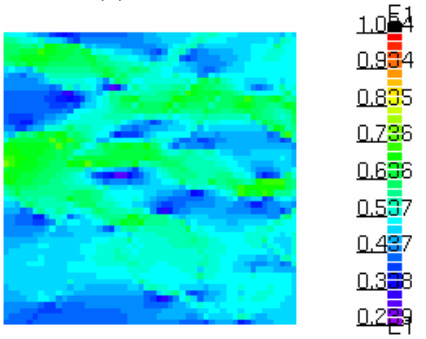

Figure 11: Mises-Stress in elements of Fig. 10b.

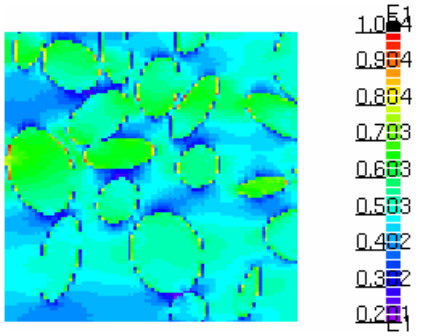

Figure 12: Stress σ_{xx} in integration points of Fig. 10b.

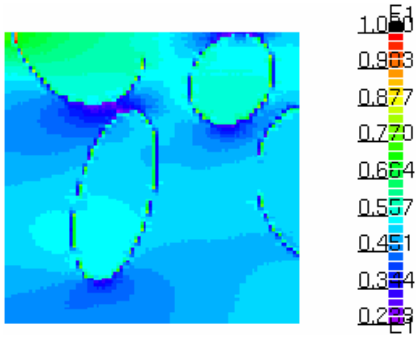

Figure 13: Stress σ_{xx} in integration points of Fig. 10c.

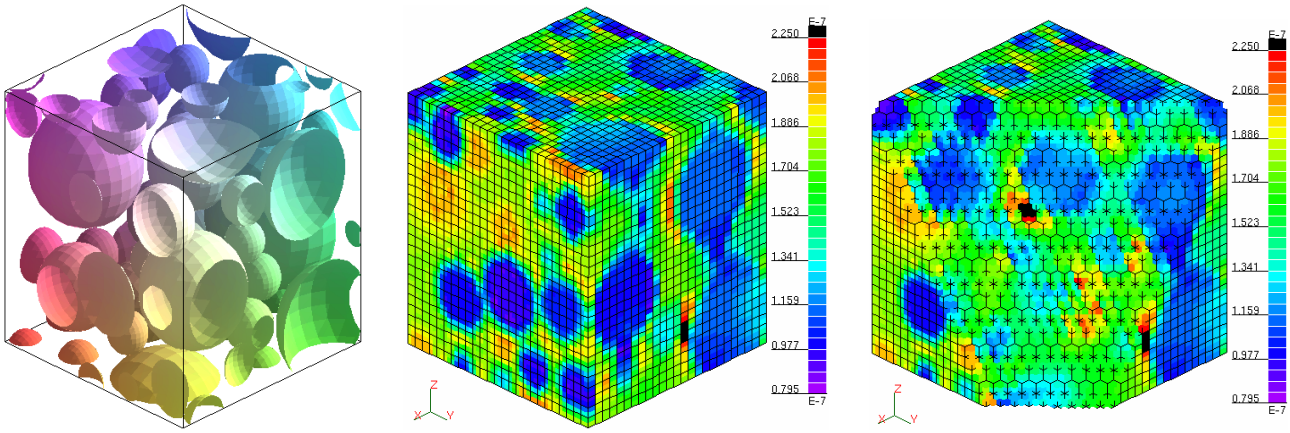

Figure 14: Extracted mesoscale geometry of $0.05 \cdot 0.05 \cdot 0.05\ m^3$ from the center of the cube shown in Fig. 9 of particle size intervall 8-32mm and corresponding strains ϵ_{xx} for a constant, external applied tension in x-direction.

4 Analysis on Multiple Scales

On regions of special interest a finer mesh is used for receiving more accurate answers about the local stress distributions. A first study of compact smooth shaped particles in a matrix showed, that for a macroscopically constant stress distribution the local stresses within the particles also only slightly vary, whereas they cause highly non-linear stresses in adjacent regions. This localized stresses within the matrix can not be detected in general by the coarse mesh of the complete geometry. However the average stress of each particle is assumed to be a good indicator where maximum stresses in the matrix occur. For the analysis of this region one or a patch of elements is replaced by a dimensionally finer, uniform mesh which is bounded by consistent displacement boundary conditions of the macroscopic model's response. Therewith a more exact analysis of the local stresses is established. Cracks can be identified and considered by just removing (or namely reducing the elastic modulus near to zero) of such small elements taking into account regularization techniques. By introducing adequate constraints the resulting effective stiffness of the former, large element is evaluated. Thereby the compatibility requirements are softened, as an edge which is crossed by a crack can no longer be described by shape function like polynomials and resisting on this would just unintentionally stiffen the element again. Consequently the crack remains sharp for the global effect and it is expected, that neighbour elements automatically adapt to each other in further iterations, as the geometrical model remains continuous and includes all previously calculated cracks.

5 Conclusions

The described concept has been established as a first prototype for the multiscale analysis of concrete based on a geometrical inclusion-matrix model. The geometrical model itself can further be adapted to better meet real constellations within concrete by fitting other algebraic formulations on analysed data of the heterogeneous structure. Better indicators and predictors of crack propagation can be introduced. Different analysis types are possible at different scales, as for example particle models, truss models [5] or inclusions with surrounded contact elements. Also the coupling of the different scales has not been completely solved. Regarding efficiency an iterative Domain Decomposition Solver can be included for uniform meshes as proposed in Ref. [11]. Besides just seeking for most efficient stand-alone algorithms the multiscale approach also requires that all algorithms match best with each other for achieving the best results at a certain time. Further enhancements will be subject of our

future research on this topic, whereas an adequate geometrical model of concrete is one of the basic approaches for a mesh independent multiscale analysis.

Acknowledgement

This research has been supported by the German Research Foundation (DFG) through *Sonderforschungsbereich 524*, which is gratefully acknowledged by the authors.

References

[1] W. Beyer. *Betonratgeber*. 2nd edition. Thomas-Beton GmbH Kiel, 1999.

[2] C. Bucher et al. SLang -*The Structural Language*. Institute of Structural Mechanics, Bauhaus-University of Weimar, Germany, 5.0 edition, 2002.

[3] W. Koensler. *Sand und Kies*. Ferdinand Enke Verlag, Stuttgart, 1989.

[4] G. Shakhmenko and J. Birsh. Concrete mix design and optimization. In *2nd Int. PhD Symposium in Civil Engineering*. Budapest, 1998.

[5] V. Slowik and J.P. De Barros Leite. Meso-level modelling of concrete fracture. Leipzig Annual Civil Engineering Report No. 5, 2000.

[6] J.G.M. van Mier. Assessment of strain softening curves for concrete. Lecture notes, Department of Civil Engineering, Delft University of Technology, 1992.

[7] Wenping Wang, Jiaye Wang, and Mying-Soo Kim. An algebraic condition for the seperation of two ellipsoids. *Computer Aided Geometric Design*, 18:531–539, 2001.

[8] D. Wenzel. Zugfestigkeit von Betonzuschlag. Studienarbeit, FA Finger-Institute for Building Material Science, Bauhaus University Weimar, 2002.

[9] T.I. Zohdi. Computational optimization of the vortex manufacturing of advanced materials. *Comput. Methods Appl. Mech. Engrg.*, 190:6231–6256, 2001.

[10] T.I. Zohdi and P. Wriggers. Aspects of computational testing of the mechanical properties of microheterogeneous material samples. *Int. J. Numer. Meth. Engng.*, 50:2573–2599, 2001.

[11] T.I. Zohdi, P. Wriggers, and C. Huet. A method of substructuring large-scale computational micromechanical problems. *Comput. Methods Appl. Mech. Engrg.*, 190:5639–5656, 2001.